Activated macrophages promote Wnt signalling through tumour necrosis factor-alpha in gastric tumour cells.

Activated macrophages promote Wnt signaling through tumor necrosis factor-α in gastric tumor cells

Keisuke Oguma[1,6], Hiroko Oshima[1,6], Masahiro Aoki[2], Ryusei Uchio[1], Kazuhito Naka[3], Satoshi Nakamura[4], Atsushi Hirao[3], Hideyuki Saya[5], Makoto Mark Taketo[2], and Masanobu Oshima[1]*

[1]Division of Genetics, Cancer Research Institute, Kanazawa University, Kanazawa, 920-0934 Japan. [2]Department of Pharmacology, Kyoto University Graduate School of Medicine, Kyoto, 606-8501 Japan. [3]Division of Molecular Genetics, Cancer Research Institute, Kanazawa University, Kanazawa, 920-0934 Japan. [4]Department of Biomedical Research and Development, Link Genomics, Tokyo, 103-0023 Japan. [5]Division of Gene Regulation, Institute for Advanced Medical Research, Keio University School of Medicine, Tokyo, 160-8582 Japan. [6]These authors contributed equally to this work.

*Corresponding author: Masanobu Oshima, Division of Genetics, Cancer Research Institute, Kanazawa University, 13-1 Takara-machi, Kanazawa, 920-0934 Japan. Tel.: +81 76 265 2721; Fax: +81 76 234 4519;
E-mail: oshimam@kenroku.kanazawa-u.ac.jp

Running title: Wnt promotion by activated macrophages

Category: “Molecular Biology of Disease”

Word count: 52,005 words including spaces

Grant Support: Grant-in-Aid for the Third-Term Comprehensive Cancer Control Strategy from the Ministry of Health, Labor and Welfare of Japan, Grant-in-Aid for Priority Areas from the Ministry of Education, Culture, Sports, Science and Technology of Japan, and Takeda Science Foundation, Japan.

Abstract

The activation of Wnt/β-catenin signaling plays a key role in gastrointestinal tumorigenesis. It has been suggested that the promotion of Wnt/β-catenin activity beyond the threshold is important for carcinogenesis. We herein investigated the role of macrophages in promotion of Wnt/β-catenin activity in gastric tumorigenesis. We found β-catenin nuclear accumulation in macrophage infiltrated dysplastic mucosa of the *K19-Wnt1* mouse stomach. Moreover, macrophage depletion in $Apc^{\Delta 716}$ mice resulted in the suppression of intestinal tumorigenesis. These results suggested the role of macrophages in the activation of Wnt/β-catenin signaling, which thus leads to tumor development. Importantly, the conditioned medium of activated macrophages promoted Wnt/β-catenin signaling in gastric cancer cells, which was suppressed by the inhibition of tumor necrosis factor (TNF)-α. Furthermore, treatment with TNF-α induces GSK3β phosphorylation, which resulted in the stabilization of β-catenin. We also found that *Helicobacter* infection in the *K19-Wnt1* mouse stomach caused mucosal macrophage infiltration and nuclear β-catenin accumulation. These results suggest that macrophage-derived TNF-α promotes Wnt/β-catenin signaling through inhibition of GSK3β, which may contribute to tumor development in the gastric mucosa.

Key words: gastric cancer / inflammation / macrophage / tumor necrosis factor-α / Wnt

Introduction

The canonical Wnt signaling pathway (Wnt/β-catenin pathway) operates by stabilizing β-catenin (Taketo, 2006). The phosphorylation of β-catenin by glycogen synthase kinase 3β (GSK3β) results in degradation through the ubiquitin pathway. The binding of Wnt ligands to a Frizzled receptor leads to inhibition of the β-catenin degradation complex consisting of APC, AXIN, and GSK3β thereby allowing the nuclear translocation of stabilized β-catenin followed by transcriptional activation of the Wnt target genes. Wnt/β-catenin signaling plays a key role in the maintenance of intestinal stem cells and progenitor cells (Korinek *et al*, 1998; van de Wetering *et al*, 2002), and its activation causes gastrointestinal tumor development (Fodde *et al*, 2001; Oshima *et al*, 1995; Oshima *et al*, 2006).

The activation level of Wnt/β-catenin signaling has been reported to be a determining factor for the multiplicity of intestinal polyposis in several types of *Apc* gene mutant mice (Gaspar and Fodde, 2004; Li *et al*, 2005). Moreover, nuclear β-catenin accumulation is predominantly observed in the invasion front of colon cancer in comparison to the non-invasive tumor area (Brabletz *et al*, 1998). Furthermore, sensitivity of embryonic stem (ES) cells for differentiation is inhibited by increase of Wntβ-catenin signaling activity (Kielman *et al*, 2002). These results, taken together, suggest that the promotion of the Wnt/β-catenin activity beyond the threshold level is required for tumorigenesis, invasion and the maintenance of cell stemness.

On the other hand, it has been established that inflammation plays an important role in cancer development (Coussens and Werb, 2002). The activation of tumor necrosis factor (TNF)-α or NF-κB pathway is required for the development of hepatocellular carcinoma (Pikarsky *et al*, 2004) and intestinal tumors (Greten *et al*, 2004; Popivanova *et al*, 2008) through the induction of growth factors and suppression of apoptosis. Although several signaling pathways have been reported for promotion of Wnt/β-catenin activity (Fodde and Brabletz, 2007), it has not been elucidated yet whether the inflammatory response contributes to the promotion of Wnt/β-catenin signaling during tumorigenesis.

Gastric cancer is the second most common cancer in the world and it is closely associated with *Helicobacter pylori* infection which leads to chronic inflammation (Correa, 2003). Moreover, the activation of the Wnt/β-catenin signaling is found in about 30% of gastric cancer (Clements *et al*, 2002), suggesting that Wnt activation is one of the major causes for gastric cancer development. We recently showed that cooperation of

Wnt signaling and prostaglandin E_2 (PGE_2) pathway causes gastric cancer development in a transgenic mouse model (Oshima *et al*, 2006). Because the activation of PGE_2 signaling induces infiltration and activation of macrophages in the gastric mucosa (Oshima *et al*, 2004; Oshima *et al*, 2005), these results collectively suggest that activated macrophages promote the Wnt/β-catenin signaling activity, which thus contributes to gastric cancer.

We herein show that TNF-α derived from activated macrophages promotes the Wnt/β-catenin activity in gastric cancer cells through the suppression of GSK3β. Moreover, *Helicobacter* infection in the *Wnt1* transgenic mice resulted in macrophage infiltration and the activation of Wnt/β-catenin signaling in the gastric mucosa, which thus led to gastric tumorigenesis. These results suggest that activated macrophages in inflammatory microenvironment play an important role in gastric tumorigenesis through the promotion of the Wnt/β-catenin activity.

Results

Macrophage infiltration and β-catenin nuclear accumulation in gastric dysplasia of K19-Wnt1 transgenic mice

K19-Wnt1 transgenic mice expressing *Wnt1* in the gastric epithelial cells develop sporadic dysplastic lesions in the glandular stomach (Oshima *et al*, 2006). In these dysplastic lesions, inflammatory cells infiltrated the submucosa, whereas cell infiltration was rarely detected in the adjacent normal mucosa (Figure 1A). By immunostaining, we found macrophage infiltration in the dysplastic mucosa, while tissue macrophages were only sparsely scattered in the normal mucosa (Figure 1B and H). We also found strong nuclear staining of β-catenin in the epithelial cells of the dysplastic mucosa (Figure 1C). Notably, β-catenin accumulated epithelial cells were physically associated with stromal macrophages in the dysplastic lesions (Figure 1E). In contrast, mild β-catenin accumulation was found only in the cell proliferation zone of the normal mucosa (Figure 1I). We confirmed the increase in the β-catenin positive index in the dysplastic lesion to be associated with the increased number of infiltrated macrophages (Figure 1F). Moreover, the number of Ki-67-positive proliferating cells increased in the dysplastic mucosa when compared with that in the adjacent normal region (Figure 1D and J). The mean Ki-67 labeling indices in the dysplastic lesions and normal mucosa were 43% and 15%, respectively ($p = 0.007$). We also confirmed by BrdU incorporation analysis that cell proliferation was increased in dysplastic lesions (Figure 1G). Based on these results, we hypothesized that macrophage infiltration by inflammatory responses causes promotion of Wnt/β-catenin signaling activity in gastric epithelial cells, which probably leads to dysplastic changes in the gastric mucosa.

Requirement of macrophages for intestinal tumor development in $Apc^{\Delta 716}$ mice

To examine whether infiltrated macrophages are required for tumorigenesis, we performed crossing experiments using *op*/*op* mice, in which the number of macrophages significantly decreased in the majority of tissues because of *Csf1* mutation (Cecchini *et al*, 1994). We first examined whether *op*/*op* mutation suppressed macrophage infiltration in the inflamed stomach using *K19-C2mE* mice, which develop gastritis with heavy macrophage accumulation (Oshima *et al,* 2004). However, mucosal macrophages were still found in the stomach of the *K19-C2mE op/op* compound mice (Supplementary Figure 1). We therefore crossed *op*/*op* mice with $Apc^{\Delta 716}$ mice, a model for intestinal

polyposis caused by Wnt activation (Oshima *et al*, 1995). *Apc*$^{\Delta 716}$ mice develop numerous polyps in entire intestinal tract (Figure 2A), and macrophages were infiltrated in the polyp stroma (Figure 2B). Interestingly, *Apc*$^{\Delta 716}$ *op*/*op* compound mice showed dramatic suppression of intestinal polyposis (Figure 2C and E), and macrophages were not found in the polyp tissues (Figure 2D). Moreover, the number of polyps > 1 mm significantly decreased in *Apc*$^{\Delta 716}$ *op*/*op* compound mice by 80% compared with *Apc*$^{\Delta 716}$ mice. Although it remains to be elucidated as to whether the loss of the CSF-1 function affects tumorigenesis, these results suggest that macrophages were required for the growth of Wnt/β-catenin-activated tumor cells. Consistently, the BrdU labeling index also decreased in *Apc*$^{\Delta 716}$ *op*/*op* mouse tumors (Figure 2F).

Fluctuation of Wnt/β-catenin signaling activity in gastric cancer cells

We next examined the regulation of the Wnt/β-catenin signaling activity by *in vitro* experiments using human gastric cancer cells, AGS and Kato-III. AGS cells harbor a heterozygous mutation in the β-catenin gene (*CTNNB1*) at codon 34 (Caca *et al*, 1999; Supplementary Figure 2), whereas *CTNNB1* is amplified in Kato-III cells (Suriano *et al*, 2005). Consistent with the previous results (Nojima *et al*, 2007), both cell lines showed an elevated β-catenin/TCF transcriptional activity as detected by a TOPFLASH assay (Supplementary Figure 3). By immunocytochemistry, the cytoplasmic and nuclear accumulation of β-catenin was found in both AGS and Kato-III cells (Figure 3A, *left*). We also found the nuclear localization of active form of β-catenin, unphosphorylated on Ser37 and Thr41 (van Noort *et al*, 2002; Figure 3A, *right*), thus indicating the activation of Wnt/β-catenin signaling. However, several cells showed a weak β-catenin staining intensity (Figure 3A, *arrowheads*), suggesting that the level of Wnt/β-catenin signaling activity varies in populations.

To examine the Wnt/β-catenin activity in the live cells, we transfected a TOPEGFP vector that expressed a green fluorescent protein (GFP) in response to β-catenin/TCF transcriptional activity (Figure 3B), and established AGS-GFP and Kato-III-GFP cell lines. We confirmed that GFP expression was induced in β-catenin accumulated cells after the transient transfection of mutant *CTNNB1* (S33A) expression vector (Figure 3C). Importantly, we directly found by time-lapse video analysis that the Wnt/β-catenin activity was not constant but fluctuated in individual AGS-GFP cells (Supplementary Video 1).

To confirm the fluctuation of Wnt/β-catenin activity, we isolated by cell sorting the high-GFP (top 5%) and low-GFP (bottom 5%) populations corresponding to high and low in Wnt/β-catenin signaling activity, respectively, from AGS-GFP and Kato-III-GFP cell (Figure 3D, *left*). Immediately after isolation, both populations showed distinct GFP intensities (Figure 3D, *center*). Importantly, however, the GFP intensities of the isolated populations returned to a similar distribution to the unsorted cells after culturing for 5 days (Figure 3D, *right*). These results confirmed that the activation level of Wnt/β-catenin signaling fluctuates in each cell.

We next examined the level of Wnt/β-catenin activity in cell cycle-synchronized Kato-III-GFP cells. However, the ratio of a high GFP population did not change during cell cycling, thus indicating Wnt/β-catenin fluctuation to be independent of the cell cycle status (Supplementary Figure 4).

Promotion of Wnt/β-catenin activity in gastric cancer cells by activated macrophages and TNF-α

We next examined whether the activity of Wnt/β-catenin signaling is promoted by activated macrophages using the GFP reporter transfected cells. We prepared a conditioned medium of macrophage cell line, RAW264, activated with lipopolysaccharide (LPS) for 24 hours [hereafter, CM-LPS (+)]. A conditioned medium from unstimulated RAW264 cells was used as the control [CM-LPS (–)]. When AGS-GFP and Kato-III-GFP cells were stimulated with CM-LPS (+), the high-GFP population (corresponding to top 2% in the untreated control cells) significantly increased in a CM concentration-dependent manner (Figure 4A and B, *left* and *top, red area*). In contrast, the stimulation of the cells with CM-LPS (–) or LPS alone did not affect the Wnt/β-catenin activity in either cell line (Figure 4A and B, *middle and bottom*). These results indicate that the soluble factor(s) derived from activated macrophages promote the Wnt/β-catenin activity in gastric cancer cells.

TNF-α is a key mediator for inflammation and is produced by activated macrophages. Notably, the treatment of the cells with a neutralizing antibody against TNF-α significantly suppressed the effect by CM-LPS (+) to enhance the Wnt/β-catenin activity in both cell lines (Figure 4C). Furthermore, direct treatment with TNF-α increased the level of Wnt/β-catenin activity (Figure 4D). We detected the expression of both TNF R1 and TNF R2 on AGS and Kato-III cells as well as in the primary cultured

gastric epithelial cells (Supplementary Figure 5A, C and data not shown). Importantly, the blockade of either receptor by neutralizing antibody significantly suppressed the TNF-α-induced Wnt/β-catenin activation (Supplementary Figure 5B). These results suggest that TNF-α signaling through both TNF R1 and TNF R2 is thus involved in the promotion of the Wnt/β-catenin activity. By immunohistochemistry, we found most TNF-α-expressing cells in gastric tumors to be macrophages, while CD11c-positive dendritic cells were rarely detected (Supplementary Figure 6A). Importantly, the treatment of the *K19-Wnt1* mice with anti-TNF-α neutralizing antibody resulted in a decrease of the β-catenin immunostaining intensity in the dysplastic lesions (Supplementary Figure 6B).

Moreover, we examined the Wnt-promoting effect of other inflammatory cytokines, IL-1β, IL-6 and IL-11, which play a role in gastric tumorigenesis (Fox and Wang, 2008; Howlett *et al*, 2005). However, these cytokines did not promote Wnt/β-catenin activity in gastric cancer cells, although IL-1β slightly increased the high-GFP population in AGS-GFP cells (Supplementary Figure 7). These results, taken together, suggest that TNF-α is one of the important macrophage-derived factors that promote the Wnt/β-catenin activity in gastric epithelial cells and cancer cells.

Suppression of β-catenin phosphorylation by TNF-α through the inhibition of GSK3β in gastric cancer cells

By a flow cytometry analysis, we found that the level of unphosphorylated β-catenin increased significantly in Kato-III cells when cells were treated with CM-LPS (+) or TNF-α (Figure 5A). By western blotting, we confirmed the increased level of unphosphorylated β-catenin in Kato-III cells stimulated with CM-LPS (+) or TNF-α (Figure 5B). These results suggested that CM-LPS (+) or TNF-α suppressed the phosphorylation of β-catenin, resulting in Wnt/β-catenin promotion. Significantly, treatment with TNF-α resulted in an increase of GSK3β phosphorylation on Ser9 both in AGS and Kato-III cells (Figure 5C), which caused the suppression of the GSK3β activity (Cross *et al*, 1995). The mean relative band intensities of the phosphorylated GSK3β to the control level were 2.03 ± 0.14 ($p = 0.009$) and 1.68 ± 0.31 ($p = 0.03$) in the AGS and Kato-III cells, respectively. Interestingly, a strong immunostaining signal for phosphorylated GSK3 was found in a subpopulation of Kato-III cells that also showed nuclear accumulation of β-catenin at the same time (Figure 5D). These results suggest that

the promotion of Wnt/β-catenin signaling is regulated by the GSK3β phosphorylation status in gastric cancer cells. Akt is an important kinase for phosphorylation of GSK3β at Ser9 (Sharma *et al*, 2002). Importantly, the active form of Akt, phosphorylated on Ser473, increased significantly after TNF-α stimulation in both AGS and Kato-III cells (Figure 5C). The mean relative band intensities of the phosphorylated Akt to the control level were 2.08 ± 0.16 (p = 0.005) and 1.81 ± 0.19 (p = 0.002) in the AGS and Kato-III cells, respectively. These results suggest that TNF-α accelerates the GSK3β phosphorylation through the activation of the Akt pathway.

NF-κB independent promotion of Wnt/β-catenin activity in gastric cancer cells

To examine whether NF-κB is involved in Wnt/β-catenin promotion by activated macrophages, we transfected IκB-superrepressor (IκBSR) expression vector into AGS-GFP cells and established two sublines, in which TNF-α-induced NF-κB activation was suppressed (Figure 6A). Notably, the TNF-α- or CM-LPS (+)-induced promotion of the Wnt/β-catenin activity did not change in either of IκBSR transfected AGS-GFP cells (Figure 6B), thus suggesting the existence of an NF-κB independent mechanism for the TNF-α-induced Wnt/β-catenin promotion.

When Kato-III cells were treated with the protein synthesis inhibitor cycloheximide, the unphosphorylated β-catenin-positive population decreased gradually in an incubation time-dependent manner, probably due to the phosphorylation of β-catenin by GSK3β (Figure 6C, *black lines*). However, the simultaneous treatment with CM-LPS (+) significantly suppressed the cycloheximide-induced decrease of this population (Figure 6C, *red lines*). Therefore, it is also possible that activated macrophages suppress β-catenin phosphorylation independent of protein synthesis, which is consistent with the results that the transcription factor NF-κB pathway is not involved in the suppression of β-catenin phosphorylation.

Macrophage infiltration and Wnt/β-catenin activation in mouse gastric epithelial cells by Helicobacter infection

We next examined whether Wnt/β-catenin signaling is activated by infection-associated inflammation in the mouse stomach. *Helicobacter felis*, a close relative to *H. pylori* was infected to *K19-Wnt1* mouse stomach. Eight weeks after *H. felis* infection, the infiltration of macrophages was found in the *H. felis*-infected gastric mucosa (Figure 7A-C), while

tissue macrophages were sparsely scattered in the non-infected mucosal area (Figure 7G-I). Such an inflamed mucosa in the infected-*K19-Wnt1* mice was only detected by histological examinations, and this inflamed mucosa was distinct from the spontaneously developed dysplastic lesions (Figure 1A). Importantly, the number of β-catenin-accumulated epithelial cells increased significantly in the infected and inflamed mucosa compared with that in the non-inflamed mucosa (Figure 7D, J, and M). These results suggest that the infection-associated inflammation promotes the Wnt/β-catenin signaling activity in gastric epithelial cells *in vivo*. Moreover, in the inflamed mucosa, the epithelial cell proliferation detected by Ki-67 immunostaining significantly increased (Figure 7E, K, and N). Furthermore, the number of H^+/K^+-ATPase-positive parietal cells decreased dramatically in the *H. felis*-infected area, thus indicating the suppression of epithelial differentiation (Figure 7F, L, and O). These results, taken together, suggest that infiltrated macrophages in response to *Helicobacter* infection play a role in the activation of Wnt/β-catenin signaling, thereby enhancing the proliferation and suppression of differentiation. When $Apc^{\Delta 716}$ mice were infected with *H. felis*, we did not find any β-catenin accumulated dysplastic cells in the inflamed gastric mucosa (data not shown). Therefore, it is possible that the basal activation level of Wnt/β-catenin signaling is required for its promotion.

Tumor development in H. felis-infected K19-Wnt1 mouse stomach

We finally examined whether *H. felis* infection contributes to gastric tumorigenesis in *K19-Wnt1* mice. Importantly, *K19-Wnt1* mice developed gastric tumors at 20 weeks after *H. felis* infection, while no tumors were found in the *H. felis*-infected wild-type mice (Figure 8A, E). Histologically, submucosal infiltration was found in both *H. felis*-infected *K19-Wnt1* and wild-type mouse stomach (Figure 8B, F). Although macrophage infiltration was detected in both genotypes (Figure 8C, G), dysplastic epithelial cells were evident in the infected *K19-Wnt1* tumors but not in the wild-type mouse stomach (Figure 8D, H). These results, taken together, suggest that infection-associated inflammation plays a role in gastric tumorigenesis through the promotion of the Wnt/β-catenin activity beyond the basal activation level.

Discussion

Macrophage infiltration and cancer development, progression and stemness

The activation of Wnt/β-catenin signaling by genetic alteration, such as mutation in *APC* or *CTNNB1*, is responsible for gastrointestinal tumorigenesis. However, accumulating evidence suggests that further promotion of the Wnt/β-catenin activity plays an important role in tumor growth and progression (Fodde and Brabletz, 2007). For example, increased β-catenin accumulation is found in the invasion front of colon cancer (Brabletz *et al*, 1998). We herein demonstrated direct evidence that the Wnt/β-catenin activity fluctuates in individual cancer cells that carry the same genetic alteration in *CTNNB1*. Accordingly, Wnt/β-catenin signaling can be promoted beyond the basal activated level by genetic alteration, and such promotion may play an important role in both tumor development and progression.

We have previously shown the induction of COX-2/PGE_2 pathway to play a key role in the intestinal tumorigenesis that is triggered by Wnt/β-catenin activation (Oshima *et al*, 1996; Sonoshita *et al*, 2001). The simultaneous induction of both Wnt and PGE_2 pathways is also responsible for gastric tumor development in mouse models (Oshima *et al*, 2006). Although PGE_2 may have multiple functions for tumorigenesis, we previously found an increased PGE_2 level to result in macrophage accumulation in the gastric mucosa of *K19-C2mE* mice (Oshima *et al*, 2004). Accordingly, it is possible that macrophage infiltration in dysplastic lesions of *K19-Wnt1* mice is caused by the spontaneous induction of COX-2/PGE_2 pathway. We herein show that Wnt/β-catenin signaling is promoted by macrophage-derived TNF-α, which contributes to gastric tumorigenesis. It is therefore possible that the induction of the COX-2/PGE_2 pathway promotes Wnt/β-catenin signaling through the enhancement of macrophage infiltration, which is responsible for tumor development.

On the other hand, Wnt/β-catenin signaling is not activated in the stomach of either *K19-C2mE* mice or *H. felis*-infected $Apc^{\Delta 716}$ mice, thus indicating that the induction of the COX-2/PGE_2 pathway and subsequent macrophage infiltration are not sufficient for the promotion of Wnt/β-catenin in gastric epithelial cells. It is conceivable that the basal activation of the Wnt/β-catenin pathway by genetic alteration is required for the promotion of Wnt/β-catenin signaling.

The activation of Wnt/β-catenin pathway is also suggested to be important for stemness. Wnt/β-catenin signaling is required for the maintenance of normal intestinal

stem cells (Korinek *et al*, 1998), and the increase in the Wnt/β-catenin activity contributes to the maintenance of stemness in embryonic stem cells (Kielman *et al*, 2002). Accordingly, it is possible that the increased Wnt/β-catenin activity is also important for the maintenance of cancer stem cells. Therefore, infiltrated macrophages in tumor tissues may be an important component of niche for cancer stem cells by promoting Wnt/β-catenin signaling through TNF-α pathway. This hypothesis is supported by the results that macrophages are required for the maintenance of progenitor cells in the intestinal crypt (Pull *et al*, 2005).

Other possible pathways than TNF-α for the promotion of the Wnt/β-catenin signaling activity

It has been shown that inflammatory cytokines, TNF-α, IL-1β, IL-6 or IL-11, play an important role in gastric tumorigenesis (Fox and Wang, 2007; Howlett *et al*, 2005). Among these cytokines, TNF-α is the most potent Wnt/β-catenin promoting factor, although IL-1β slightly increases Wnt signaling in AGS cells. However, the increased level of the Wnt/β-catenin activity by CM-LPS (+) is significantly higher than that by TNF-α alone in both cell lines (Figure 4), thus suggesting the effect of other macrophage-derived factors on Wnt/β-catenin promotion. It has been reported that hepatocyte growth factor (HGF) activates Wnt/β-catenin signaling through the tyrosine phosphorylation of β-catenin (Rasola *et al*, 2006), and platelet-derived growth factor (PDGF) also promote Wnt/β-catenin signaling through suppression of β-catenin phosphorylation (Yang *et al*, 2006). It is therefore possible that these factor(s) contribute to Wnt/β-catenin promotion together with TNF-α in gastric tumorigenesis.

Recently, using a colon tumor mouse model, TNF R1 signaling in bone marrow-derived cells has been shown to indirectly enhance epithelial Wnt/β-catenin signaling (Popivanova *et al*, 2008). Accordingly, it is possible that TNF-α signaling, not only in epithelial cells but also in stromal cells, may therefore contribute to the promotion of Wnt/β-catenin signaling in cancer cells.

Promotion of Wnt/β-catenin signaling in cancer cells that retain wild-type CTNNB1

We show here that TNF-α stimulation promotes the Wnt/β-catenin signaling activity through the suppression of β-catenin phosphorylation by GSK3β. Therefore, the expression of wild-type β-catenin is required for the promotion of Wnt/β-catenin signaling

in epithelial cells as well as cancer cells. Because Kato-III cells have a multicopy of the wild-type *CTNNB1* (Suriano *et al*, 2005), TNF-α stimulation suppresses phosphorylation of these β-catenin, thus leading to the enhancement of Wnt/β-catenin signaling. On the other hand, AGS cells possess mutation in *CTNNB1* close to the phosphorylation site of GSK3β (Supplementary Figure 1; Caca *et al*, 1999), which causes the activation of the basal Wnt/β-catenin signaling. It is therefore possible that TNF-α stimulation suppresses phosphorylation of wild-type β-catenin expressed from retained intact *CTNNB1*, which contributes to the promotion of the total Wnt/β-catenin activity of AGS cells. In human gastric cancer, a *CTNNB1* mutation is found in about 30% of the Wnt-activated cases (Clements *et al*, 2002). However, either a somatic mutation or downregulation of E-cadherin (Cheng *et al*, 2005), secreted frizzled-related proteins (Nojima *et al*, 2007), or β-TrCP, a component of ubiquitin ligase complex (Kim *et al*, 2007) is found in gastric cancer, which leads to the basal activation of Wnt/β-catenin signaling without mutation in *CTNNB1*. These results, taken together, suggest that wild-type β-catenin expressed in gastric cancer cells is stabilized by inflammatory macrophages thus resulting in the promotion of Wntβ-catenin signaling, which contributes to cancer development, progression and the maintenance of cancer stem cells.

Accordingly, the present results suggest that the suppression of macrophage infiltration and its activation by anti-inflammatory drugs or inhibitors for PGE_2 pathway is therefoe a possible strategy for chemoprevention against gastric cancer.

Materials and Methods

Animal experiments

The construction of *K19-Wnt1* and *K19-C2mE* transgenic mice has been described previously (Oshima *et al*, 2004; Oshima *et al*, 2006). Briefly, *K19-Wnt1* mice express *Wnt1*, while *K19-C2mE* mice express COX-2 and mPGES-1 in gastric epithelial cells under transcriptional regulation by cytokeratin 19 (K19) gene promoter. *K19-Wnt1* transgenic mice were euthanized at 30 weeks of age (n=10), and the glandular stomach was fixed with 4% paraformaldehyde and processed for histological analysis. *Helicobacter felis* (ATCC49179) was cultured as previously described (Oshima *et al*, 2004). *H. felis* bacteria were inoculated at 10^8/mouse *p.o.* to *K19-Wnt* mice, $Apc^{\Delta 716}$ mice (Oshima *et al*, 1995), and wild-type mice. The infected *K19-Wnt1* mice were examined at 8 weeks and 20 weeks after the *H. felis* inoculation (n=3 for each mice). The infected $Apc^{\Delta 716}$ mice were examined at 6 weeks after infection (n=4). The localization of *H. felis*-infected mucosa at 8 weeks was estimated by the detection of bacteria using microscope with X100 objective (Figure 7B). $Apc^{\Delta 716}$ mice were crossed with *op*/*op* mice (The Jackson Laboratory) to obtain $Apc^{\Delta 716}$ *op*/*op* compound mice (n=3) and littermate control $Apc^{\Delta 716}$ mice (n=3). The intestine of $Apc^{\Delta 716}$ and $Apc^{\Delta 716}$ *op*/*op* mice was examined at 12 weeks of age, and the total number of polyps was determined using a dissecting microscope. For scoring the BrdU labeling index, the mice were injected *i.p.* with 200 μl of BrdU solution (Roche) and then the tissue specimens were processed for immunostaining using anti-BrdU antibody. All animal experiments were carried out according to the protocol approved by the Committee on Animal Experimentation of Kanazawa University.

Histology and immunostaining

The stomach tissues were fixed in 4% paraformaldehyde, paraffin-embedded, and sectioned at 4 μm-thickness. These sections were stained with H&E. Serial sections were immunostained with antibodies for Ki-67 (DakoCytomation), F4/80 (Serotec), unphosphorylated (activated) β-catenin on Ser37 and Thr41 (Upstate), H^+/K^+-ATPase (MBL, Nagoya, Japan), or BrdU (Roche) as the primary antibody. The staining signals were visualized using the Vectorstain Elite Kit (Vector Laboratories). The number of positive stained cells for F4/80, β-catenin, Ki-67, or H^+/K^+-ATPase was scored in 20 randomly selected gastric glands and the mean values were calculated. The number of

BrdU positive cells and the total number of nuclei was counted in five microscopic fields and then the mean value was calculated as the BrdU labeling index. For immunofluorescence staining, Alexa Fluor 594 donkey anti-mouse IgG or Alexa Fluor 488 anti-rat or rabbit IgG (Molecular Probes) was used as the secondary antibody.

Plasmid vector construction

For the construction of the β-catenin/TCF reporter plasmid with GFP (TOPEGFP vector), cDNA encoding EGFP was excised from pIRES2-EGFP (Clontech) and replaced with luciferase gene in TOPFLASH plasmid (Upstate). TOPEGFP reporter plasmid was transfected to cells using Effectene Transfection Reagent (QIAGEN), and stable cell lines were then obtained by cell sorting. The Wnt/β-catenin activity using TOPEGFP reporter was measured by flow cytometry (*see below*). pcDNA3-S33A-β-catenin and pBSFI-IκB-SR (IκB-Superrepressor) plasmids were kindly provided by Dr. Peter Vogt at the Scripps Research Institute. pcDNA3-S33A-β-catenin was transiently transfected to Kato-III-GFP cells for 72 hours to express stabilized mutant β-catenin. pBSFI-IκB-SR was transfected to AGS-GFP cells to establish the sublines in which the NF-κB pathway is suppressed.

Immunocytochemistry

Gastric cancer cells grown on cover slips were fixed with 10% neutral buffered formalin and permeabilized with 0.1% Triton X-100 in PBS. Anti-total β-catenin antibody (Sigma), anti-unphosphorylated β-catenin antibody (Upstate), or anti-phosphorylated GSK3 (Cell Signaling) was used as the primary antibody, and anti-mouse IgG Alexa 594 or anti-rat IgG Alexa 488 (Molecular Probes) were used as the secondary antibody. Next, cover slips were mounted using VECTASHIELD Mounting Medium (Vector laboratories) that contained DAPI for nuclear staining.

Cell culture and preparation of conditioned medium

Gastric cancer cell lines, AGS (ATCC) and Kato-III (Cell Resource Center for Biomedical Research, Tohoku Univ., Japan) were cultured in RPMI1640 medium supplemented with 10% FBS in a humidified incubator at 37^0C with 5% CO_2. The mouse macrophage cell line RAW264 (RIKEN BioResource Center, Tsukuba, Japan) was cultured in RPMI1640, and treated with LPS purified from *Salmonella enterica* serotype

typhimurium (Sigma) at 100 ng/ml for 24 h. The conditioned medium, CM-LPS (+) was collected and used for the Wnt/β-catenin activation experiments. The control conditioned medium, CM-LPS (–) was prepared from non-stimulated RAW264 cell culture. For either the stimulation or inhibition of the TNF-α pathway, TNF-α (Calbiochem) or anti-mouse TNF-α neutralizing antibody (R&D systems) was added, respectively, in the culture medium at the indicated concentration.

NF-κB ELISA assay

The nuclear extract was prepared from AGS-GFP cells or pBSFI-IκB-SR-transrected clones (IκBSR #1 and #2) using NE-PER Nuclear Extraction Reagents (Pierce), and the NF-κB activity was measured using an NF-κB p65 Transcription Factor Assay Kit (Active Motif). These cell lines were also used for the flow cytometry analysis.

Flow cytometry analysis

After treatment with CM-LPS (+), CM-LPS (-), LPS, or TNF-α at the indicated concentrations for 48 h, AGS-GFP, Kato-III-GFP cells or pBSFI-IκB-SR transfected cells (IκBSR #1 and #2) were washed with PBS containing 2% FCS and stained with 5 μg/ml propidium iodide to exclude dead cells. GFP fluorescence was examined with FACSCalibur (Becton Dickinson). A fluorescence intensity corresponding to the top 2% of the control untreated cells was judged as the high-GFP population (high-Wnt/β-catenin signaling population).

For the analysis of intracellular unphosphorylated (active) β-catenin, cells were fixed in 1-2% paraformaldehyde and permeabilized using 0.05% Triton X-100 in PBS containing 2% FCS. Next, the cells were incubated with anti-unphosphorylated β-catenin antibody on Ser37 and Thr41 (Upstate) followed by anti-mouse IgG-Alexa 488 (Molecular probes), and examined with FACSCalibur. For the inhibition of protein translation, the cells were treated with cycloheximide (Sigma) at 0.5 μg/ml for the indicated time, and then the intracellular unphosphorylated β-catenin was measured by a FACS analysis as described above.

Western blotting analysis

For the detection of total β-catenin and unphosphorylated β-catenin, the cells were stimulated with CM-LPS (+) or TNF-α at 10 ng/ml for 24 h. For the detection of total or

phosphorylated GSK3β (Ser9), and phosphorylated Akt (Ser473), the cells were cultured in serum free conditions for 24 h followed by stimulation with TNF-α at 100 ng/ml for 24 h. Next, the cells were lysed and sonicated in lysis buffer. After centrifugation at 20,000 × g, 10 μg of the supernatant protein was separated in a 10% SDS-polyacrylamide gel. Antibodies for unphosphorylated (active) β-catenin (Upstate), total β-catenin (Sigma), total GSK3β (BD Biosciences), phosphorylated GSK3 on Ser9 and 21 (Cell Signaling), and phosphorylated Akt at Ser473 (Cell Signaling) were used as the primary antibody. β-Actin was used as an internal control. The ECL detection system (Amersham Biosciences) was used to detect specific signals.

Statistical analysis

The data were analyzed by the paired or unpaired *t*-test using Microsoft Excel (Microsoft). A value of $p < 0.05$ was accepted as statistically significant.

Acknowledgement

We thank Manami Watanabe for her valuable technical contribution. This work was supported by Grant-in-Aid for the Third-Term Comprehensive Cancer Control Strategy from the Ministry of Health, Labor and Welfare of Japan, Grant-in-Aid for Priority Areas from the Ministry of Education, Culture, Sports, Science and Technology of Japan, and Takeda Science Foundation, Japan.

References

Brabletz T, Jung A, Hermann K, Günther K, Hohenberger W, Kirchner T (1998) Nuclear overexpression of the oncoprotein β-catenin in colorectal cancer is localized predominantly at the invasion front. *Pathol Res Pract* **194:** 701-704

Caca K, Kolligs FT, Ji X, Hayes M, Qian J, Yahanda A, Rimm DL, Costa J, Fearon ER (1999) β- and γ-catenin mutations, but not E-cadherin inactivation, underlie T-cell factor/lymphoid enhancer factor transcriptional deregulation in gastric and pancreatic cancer. *Cell Growth Differ* **10:** 369-376

Cecchini MG, Dominguez MG, Mocci S, Wetterwald A, Felix R, Fleisch H, Chisholm O, Hofstetter W, Pollard JW, Stanley ER (1994) Role of colony stimulating factor-1 in the establishment and regulation of tissue macrophages during postnatal development of the mouse. *Development* **120:** 1357-1372

Cheng XX, Wang ZC, Chen XY, Sun Y, Kong QY, Liu J, Li H (2005) Correlation of Wnt-2 expression and β-catenin intracellular accumulation in Chinese gastric cancers: relevance with tumour dissemination. *Cancer Lett* **223:** 339-347

Clements WM, Wang J, Sarnaik A, Kim OJ, MacDonald J, Fenoglio-Preiser C, Groden J, Lowy AM (2002) *β-Catenin* mutation is a frequent cause of Wnt pathway activation in gastric cancer. *Cancer Res* **62:** 3503-3506

Correa P (2003) *Helicobacter pylori* infection and gastric cancer. *Cancer Epidemiol Biomarkers Prev* **12:** 238s-241s

Coussens LM, Werb Z (2002) Inflammation and cancer. *Nature* **420:** 860-867

Cross DA, Alessi DR, Cohen P, Andjelkovich M, Hemmings BA (1995) Inhibition of glycogen synthase kinase-3 by insulin mediated by protein kinase B. *Nature* **378:** 785-789

Fodde R, Smits R, Clevers H (2001) *APC*, signal transduction and genetic instability in colorectal cancer. *Nat Rev Cancer* **1:** 55-67

Fodde R, Brabletz T (2007) Wnt/β-catenin signaling in cancer stemness and malignant behavior. *Curr Opin Cell Biol* **19:** 150-158

Fox JG, Wang TC (2008) Inflammation, atrophy and gastric cancer. *J Clin Invest* **117:** 60-69

Gaspar C, Fodde R (2004) *APC* dosage effects in tumorigenesis and stem cell differentiation. *Int J Dev Biol* **48:** 377-386

Greten FR, Eckmann L, Greten TF, Park JM, Li ZW, Egan LJ, Kagnoff MF, Karin M

(2004) IKKβ links inflammation and tumorigenesis in a mouse model of colitis-associated cancer. *Cell* **118:** 285-296

Howlett M, Judd LM, Jenkins B, La Gruta NL, Grail D, Ernst M, Giraud AS (2005) Differential regulation of gastric tumor growth by cytokines that signal exclusively through the coreceptor gp130. *Gastroenterol* **129:** 1005-1018

Kielman MF, Ridanpää M, Gaspar C, van Poppel N, Breukel C, van Leeuwen S, Taketo MM, Roberts S, Smits R, Fodde R (2002) *Apc* modulates embryonic stem-cell differentiation by controlling the dosage of β-catenin signaling. *Nat Genet* **32:** 594-605

Kim CJ, Song JH, Cho YG, Kim YS, Kim SY, Nam SW, Yoo NJ, Lee JY, Park WS (2007) Somatic mutations of the *β-TrCP* gene in gastric cancer. *APMIS* **115:** 127-133

Korinek V, Barker N, Moerer P, van Donselaar E, Huls G, Peters PJ, Clevers H (1998) Depletion of epithelial stem-cell compartments in the small intestine of mice lacking Tcf-4. *Nat Genet* **19:** 379-383

Li Q, Ishikawa TO, Oshima M, Taketo MM (2005) The threshold level of adenomatous polyposis coli protein for mouse intestinal tumorigenesis. *Cancer Res* **65:** 8622-8627

Nojima M, Suzuki H, Toyota M, Watanabe Y, Maruyama R, Sasaki S, Sasaki Y, Mita H, Nishikawa N, Yamaguchi K, Hirata K, Itoh F, Tokino T, Mori M, Imai K, Shinomura Y (2007) Frequent epigenetic inactivation of *SFRP* genes and constitutive activation of Wnt signaling in gastric cancer. *Oncogene* **26:** 4699-4713

Oshima M, Oshima H, Kitagawa K, Kobayashi M, Itakura C, Taketo M (1995) Loss of *Apc* heterozygosity and abnormal tissue building in nascent intestinal polyps in mice carrying a truncated *Apc* gene. *Proc Natl Acad Sci USA* **92:** 4482-4486

Oshima M, Dinchuk JE, Kargman SL, Oshima H, Hancock B, Kwong E, Trzaskos JM, Evans JF, Taketo MM (1996) Suppression of intestinal polyposis in $Apc^{\Delta 716}$ knockout mice by inhibition of cyclooxygenase 2 (COX-2). *Cell* **87:** 803-809

Oshima H, Oshima M, Inaba K, Taketo MM (2004) Hyperplastic gastric tumors induced by activated macrophages in COX-2/mPGES-1 transgenic mice. *EMBO J* **23:** 1669-1678

Oshima M, Oshima H, Matsunaga A, Taketo MM (2005) Hyperplastic gastric tumors with spasmolytic polypeptide-expressing metaplasia caused by tumor necrosis factor-α-dependent inflammation in cyclooxygenase-2/microsomal prostaglandin E

synthase-1 transgenic mice. *Cancer Res* **65:** 9147-9151

Oshima H, Matsunaga A, Fujimura T, Tsukamoto T, Taketo MM, Oshima M (2006) Carcinogenesis in mouse stomach by simultaneous activation of the Wnt signaling and prostaglandin E_2 pathway. *Gastroenterology* **131:** 1086-1095

Pikarsky E, Porat RM, Stein I, Abramovitch R, Amit S, Kasem S, Gutkovich-Pyest E, Urieli-Shoval S, Galun E, Ben-Neriah Y (2004) NF-κB functions as a tumour promoter in inflammation-associated cancer. *Nature* **431:** 461-466

Popivanova BK, Kitamura K, Wu Y, Kondo T, Kagaya Y, Kaneko S, Oshima M, Fujii C, Mukaida N (2008) Blocking TNF-α in mice reduces colorectal carcinogenesis associated with chronic colitis. *J Clin Invest* **118:** 560-570

Pull SL, Doherty JM, Mills JC, Gordon JI, Stappenbeck TS (2005) Activated macrophages are an adaptive element of the colonic epithelial progenitor niche necessary for regenerative responses to injury. *Proc Natl Acad Sci USA* **102:** 99-104

Rasola A, Fassetta M, De Bacco F, D'Alessandro L, Gramaglia D, Di Renzo MF, Comoglio PM (2006) A positive feedback loop between hepatocyte growth factor receptor and β-catenin sustains colorectal cancer cell invasive growth. *Oncogene* **26:** 1078-1087

Sharma M, Chuang WW, Sun Z (2002) Phosphatidylinositol 3-kinase/Akt stimulates androgen pathway through GSK3β inhibition and nuclear β-catenin accumulation. *J Biol Chem* **277:** 30935-30941

Sonoshita M, Takaku K, Sasaki N, Sugimoto Y, Ushikubi F, Narumiya S, Oshima M, Taketo MM (2001) Acceleration of intestinal polyposis through prostaglandin receptor EP2 in *Apc*$^{\Delta 716}$ knockout mice. *Nat Med* **7:** 1048-1051

Suriano G, Vrcelj N, Senz J, Ferreira P, Masoudi H, Cox K, Nabais S, Lopes C, Machado JC, Seruca R, Carneiro F, Huntsman DG (2005) β-catenin (*CTNNB1*) gene amplification: A new mechanism of protein overexpression in cancer. *Genes Chromosomes Cancer* **42:** 238-246

Taketo MM (2006) Wnt signaling and gastrointestinal tumorigenesis in mouse models. *Oncogene* **25:** 7522-7530

van Noort M, Meeldijk J, van der Zee R, Destree O, Clevers H (2002) Wnt signaling controls the phosphorylation status of β-catenin. *J Biol Chem* **277:** 17901-17905

van de Wetering M, Sancho E, Verweij C, de Lau W, Oving I, Hurlstone A, van der Horn K, Batlle E, Coudreuse D, Haramis AP, Tjon-Pon-Fong M, Moerer P, van den Born

M, Soete G, Pals S, Eilers M, Medema R, Clevers H (2002) The β-catenin/TCF-4 complex imposes a crypt progenitor phenotype on colorectal cancer cells. *Cell* **111:** 241-250

Yang L, Lin C, Liu ZR (2006) P68 RNA helicase mediates PDGF-induced epithelial mesenchymal transition by displacing Axin from β-catenin. *Cell* **127:** 139-155

Figure Legends

Figure 1. Macrophage accumulation and nuclear localization of β-catenin in dysplastic lesion of the *K19-Wnt1* mouse stomach. (**A**) Representative histology of a dysplastic lesion in the *K19-Wnt1* glandular stomach (H&E staining). The arrowheads indicate the dysplastic mucosal area. The arrows indicate submucosal inflammatory infiltration. High-magnifications of boxed area (*D*, dysplastic lesion; and *N*, adjacent normal mucosa) in serial sections are shown in (**B-E, G**) and (**H-J**), respectively. Immunostaining results for macrophage marker F4/80 (**B, H**), β-catenin (**C, I**), Ki-67 (**D, J**), and BrdU (**G**) are shown. The arrowheads in (**B, H**) indicate mucosal macrophages. The inset in (**C**) indicates the nuclear localization of β-catenin in epithelial cells, while the inset in (**I**) indicates weak cytoplasmic accumulation of β-catenin. The arrows in (**D**, **G**) indicate proliferating cells that are positive for Ki-67 and BrdU, respectively. (**E**) Double immunofluorescence staining for F4/80 (*red*) and β-catenin (*green*) in dysplastic lesion. Arrowheads indicate macrophages. (**F**) The mean ratio of β-catenin accumulated epithelial cells and the mean number of infiltrated macrophages per field in the dysplastic lesion and adjacent normal mucosa. The arrows in (**I, J**) indicate normal progenitor cells localized in gland neck with mild accumulation of β-catenin and positive Ki-67 staining. Bars indicate 100 μm.

Figure 2 Suppression of intestinal tumorigenesis by depletion of macrophages. (**A**, **C**) Representative photographs of small intestine of $Apc^{\Delta 716}$ mice (*A*) and $Apc^{\Delta 716}$ *op/op* compound mutant mice (*C*) were taken using a dissecting microscope. The arrowheads indicate intestinal polyps. Bars indicate 2 mm. (**B**, **D**) F4/80 macrophage immunostaining of polyp tissues in $Apc^{\Delta 716}$ (*B*) and $Apc^{\Delta 716}$ *op/op* compound mice (*D*). The arrows indicate macrophages. Bars indicate 100 μm. (**E**) The number of total polyps and large polyps > 1 mm in diameter of $Apc^{\Delta 716}$ (*cont*) and $Apc^{\Delta 716}$ *op/op* compound mice (*op/op*) are shown as mean ± s.d. (**F**) BrdU labeling index in polyps of $Apc^{\Delta 716}$ (*cont*) and $Apc^{\Delta 716}$ *op/op* mice (*op/op*) are shown as mean ± s.d. The asterisks indicate $p < 0.05$ in comparison to the control.

Figure 3 Fluctuation of the Wnt/β-catenin activity in gastric cancer cells. (**A**) Representative results of immunocytochemistry of AGS (*top panels*) and Kato-III (*bottom panels*) using anti-total β-catenin antibody (green) and DAPI (blue) (*left panels*)

or anti-unphosphorylated β-catenin antibody (red) (*right panels*) of the same specimen. The arrows indicate cells with accumulated both total and unphosphorylated β-catenin. The arrowheads indicate cells with weak or loss of β-catenin staining. (**B**) Construction of TOPEGFP expression vector. EGFP cDNA was inserted between TCF binding site/TK minimum promoter and SV40 pA signal. (**C**) Representative results of immunocytochemistry of Kato-III-GFP cells transiently transfected with pcDNA3-S33A-β-catenin for 72 h. GFP expression (green) with DAPI staining (blue) (*left panel*), and unphosphorylated β-catenin (red) of the same specimen (*right panel*) are shown. The arrows indicate the cell cluster with elevated GFP and unphosphorylated β-catenin levels. (**D**) Representative results of flow cytometry for GFP fluorescence of AGS-GFP (*top*) and Kato-III-GFP (*bottom*) cells. Flow cytometry results of the isolated high GFP (top 5%, red line) and low GFP (bottom 5%, blue line) populations at 0 h (*center*) and 5 days (*right*) after isolation by cell sorting.

Figure 4 Enhancement of Wnt/β-catenin signaling by the activated macrophages in gastric cancer cells. (**A, B**) Representative results of flow cytometry of AGS-GFP (*A*) and Kato-III-GFP cells (*B*). The cells were treated with CM-LPS (+) (*top*), CM-LPS (–) (*middle*), or LPS alone (*bottom*) at various concentrations indicated on top of each panel. The red area in each panel indicates a population with a high GFP intensity corresponding to the top 2% of the control cells (*left*). The percentage of high GFP population (red area) is indicated in each panel. (**C**) Representative flow cytometry of AGS-GFP (*top*) and Kato-III-GFP (*bottom*) treated with CM-LPS (+) alone (*center*) or CM-LPS (+) with anti-TNF-α neutralizing antibody (*right*). The percentage of a high-GFP population (red area corresponding to top 2% in control cells, *left*) is indicated in each panel. (**D**) Representative flow cytometry results of AGS-GFP (*top*) and Kato-III-GFP (*bottom*) treated with TNF-α (*red lines*) and untreated control (*black lines*). The percentage of high-GFP in TNF-α treated cells (corresponding to top 2% in control cells, *gray area*) is indicated in each panel.

Figure 5 Suppression of β-catenin phosphorylation by CM-LPS(+) or TNF-α in gastric cancer cells. (**A**) Representative flow cytometry results of Kato-III cells using an antibody against unphosphorylated β-catenin on Ser37 and Thr41 are shown. The cells were treated with CM-LPS (+) (*center*) or TNF-α (*right*) for 24 hours. The red area

indicates population with high level of unphosphorylated β-catenin: top 10% in control cells (*left*). The percentage of red area is indicated in each panel. (**B**) Western blotting of Kato-III cells for total β-catenin (*top*) and unphosphorylated β-catenin (*middle*). The cells were treated with CM-LPS (+) (*CM*) or TNF-α at 10 ng/ml (*TNF*). β-Actin was used as internal control (*bottom*). (**C**) Western blotting of AGS cells (*left*) and Kato-III cells (*right*) for total and phosphorylated GSK3β on Ser9, and phosphorylated Akt on Ser473. β-Actin was used as an internal control. The cells were treated with TNF-α at 100 ng/ml (*TNF*) in serum free conditions. The results of three independent samples are shown for each cell line. (**D**) Representative immunocytochemistry for phosphorylated GSK3 (*p-GSK*, green) and DAPI (blue) (*left*) and unphosphorylated β-catenin (*right*) of the same specimen. The arrows indicate cells with strong staining for both p-GSK and β-catenin, while the arrowheads indicate cells with weak staining for both.

Figure 6 NF-κB independent promotion of the Wnt/β-catenin signaling activity. (**A**) The level of NF-κB activity in the TNF-α-treated (*TNF*) or untreated control (*Con.*) cells (mean ± s.d.). IκBSR #1 and #2 are AGS-GFP-derived stable transfectants with IκB superrepressor, whereas IκBSR(-) indicates parental AGS-GFP. (**B**) Representative flow cytometry results of IκBSR(-), IκBSR #1 and #2 cells (*left to right*) treated with TNF-α (*top*) or CM-LPS (+) (*bottom*) at the indicated concentrations (*red lines*). The percentage of high-GFP populations (corresponding to top 2% in untreated cells, *black lines*) is indicated in each panel. (**C**) Flow cytometry results of Kato-III cells using antibody against unphosphorylated β-catenin. The cells were treated with cycloheximide alone (*black line*) or cycloheximide and CM-LPS (+) (*red line*) for 2, 4, 8, and 12 h. The percentages of the population with high level of unphosphorylated β-catenin are indicated in each panel (*red*, cycloheximide and CM-LPS (+); *black*, cycloheximide alone).

Figure 7 The activation of Wnt/β-catenin signaling in *H. felis*-infected gastric mucosa of *K19-Wnt1* mice. (**A**-**F**) Representative histology of inflamed gastric mucosa (*IM*) of *K19-Wnt1* mice infected with *H. felis* for 8 weeks. (**G**-**L**) Non-inflamed gastric mucosal area (*NIM*) of the *K19-Wnt1* mice. H&E staining (**A**, **G**), high magnified H&E staining (**B**, **H**), immunostaining for F4/80 (**C**, **I**), unphosphorylated β-catenin (**D**, **J**), Ki-67 (**E**, **K**) and H^+/K^+-ATPase (**F**, **L**). Bars in (*B, H*) and other panels indicate 50 μm and 100 μm, respectively. The arrows in (**A**) and (**C**) indicate infiltrated mononuclear cells and

macrophages, respectively. The yellow arrowheads in (**B**) indicate *Helicobacter* bacteria in the gland lumen, which is not found in NIM (**H**). The arrows in (**D**) and (**E**) indicate β-catenin accumulated and proliferating epithelial cells, respectively. The arrows in (**F**) indicate H^+/K^+-ATPase-positive parietal cells that are dramatically decreased in IM compared with NIM (**L**). The arrows in (**J**) and (**K**) indicate progenitor cells with cytoplasmic β-catenin accumulation and Ki-67-positive proliferation. The mean numbers of positive cells per gland for unphosphorylated β-catenin (**M**), Ki-67 (**N**), and H^+/K^+-ATPase (**O**) in IM (*red bars*) and NIM (*blue bars*) are shown as histograms (mean ± s.d.). The asterisks indicate $p < 0.05$.

Figure 8 Tumor development in *H. felis*-infected *K19-Wnt1* mouse stomach. *K19-Wnt1* (**A**-**D**) and wild-type (**E**-**H**) mouse stomach infected with *H. felis* for 20 weeks. (**A**, **E**) Macroscopic photographs. The arrows in (**A**) indicate gastric tumors which developed in the infected *K19-Wnt1* mice. H&E staining at low magnification (**B**, **F**) and high magnification (**D**, **H**). Immunostaining results for macrophage marker F4/80 (**C**, **G**). The arrows in (**B**, **F**) indicate submucosal infiltration. The arrowheads in (**D**) indicate dysplastic epithelial cells. Bars in (*B, F*) and (*C, D, G, H*) indicate 200 μm and 40 μm, respectively.

Figure 1

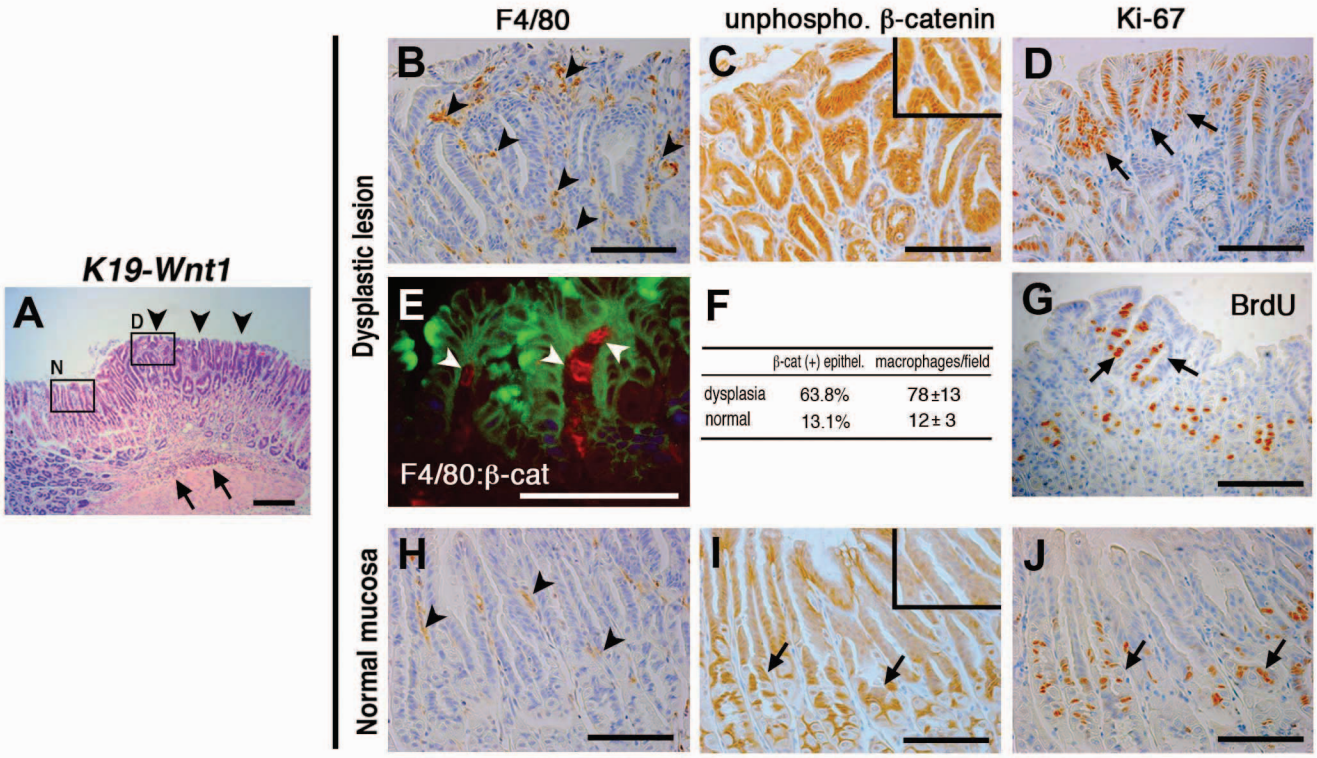
K19-Wnt1
A
D
N
F4/80
unphospho. β-catenin
Ki-67
Dysplastic lesion
B
C
D
E
F4/80:β-cat
F
β-cat (+) epithel.
macrophages/field
dysplasia
63.8%
78±13
normal
13.1%
12± 3
G
BrdU
Normal mucosa
H
I
J

Figure 2

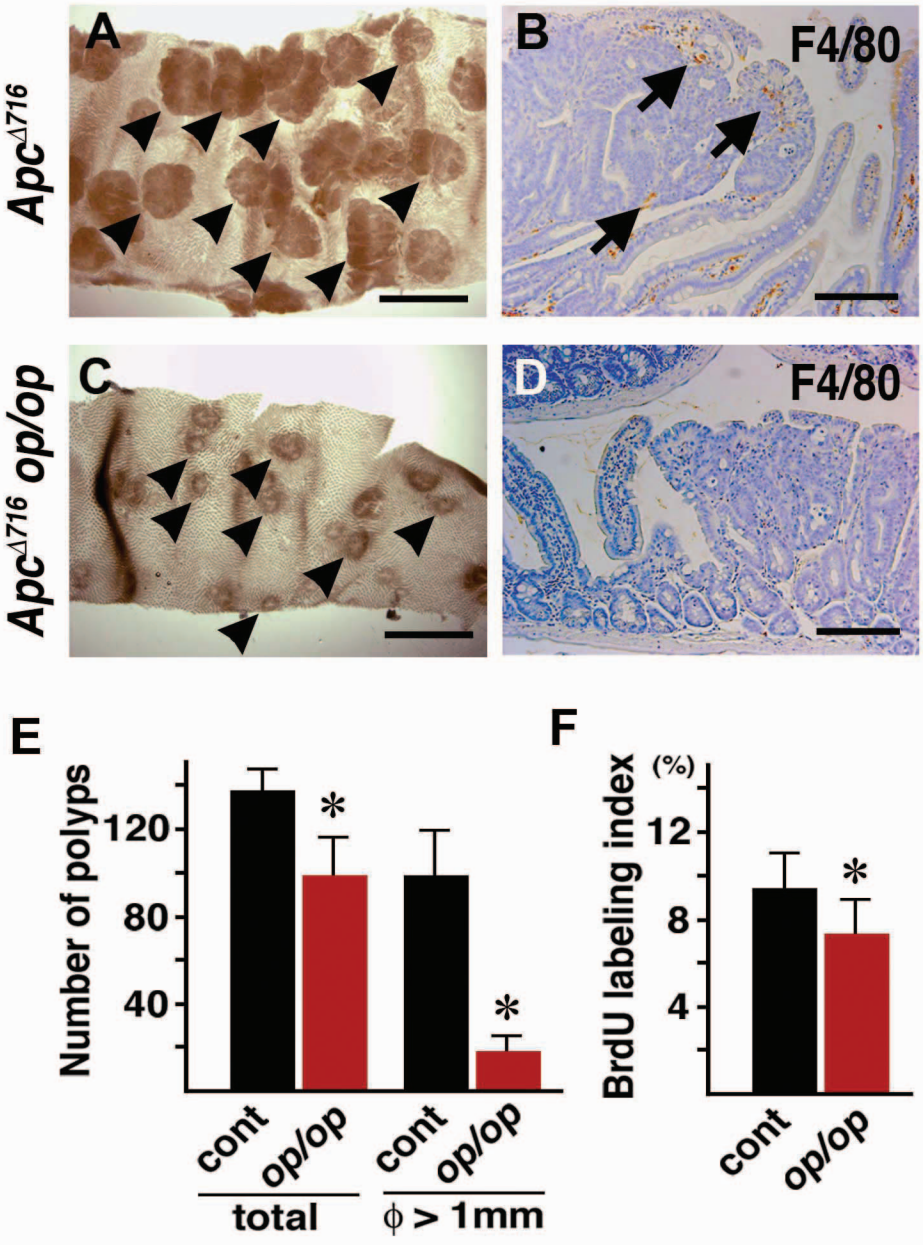
A
B
F4/80
Apc^Δ716
C
D
F4/80
Apc^Δ716 op/op
E
Number of polyps
120
80
40
*
*
cont
op/op
cont
op/op
total
ϕ > 1mm
F
BrdU labeling index
(%)
12
8
4
*
cont
op/op

Figure 3

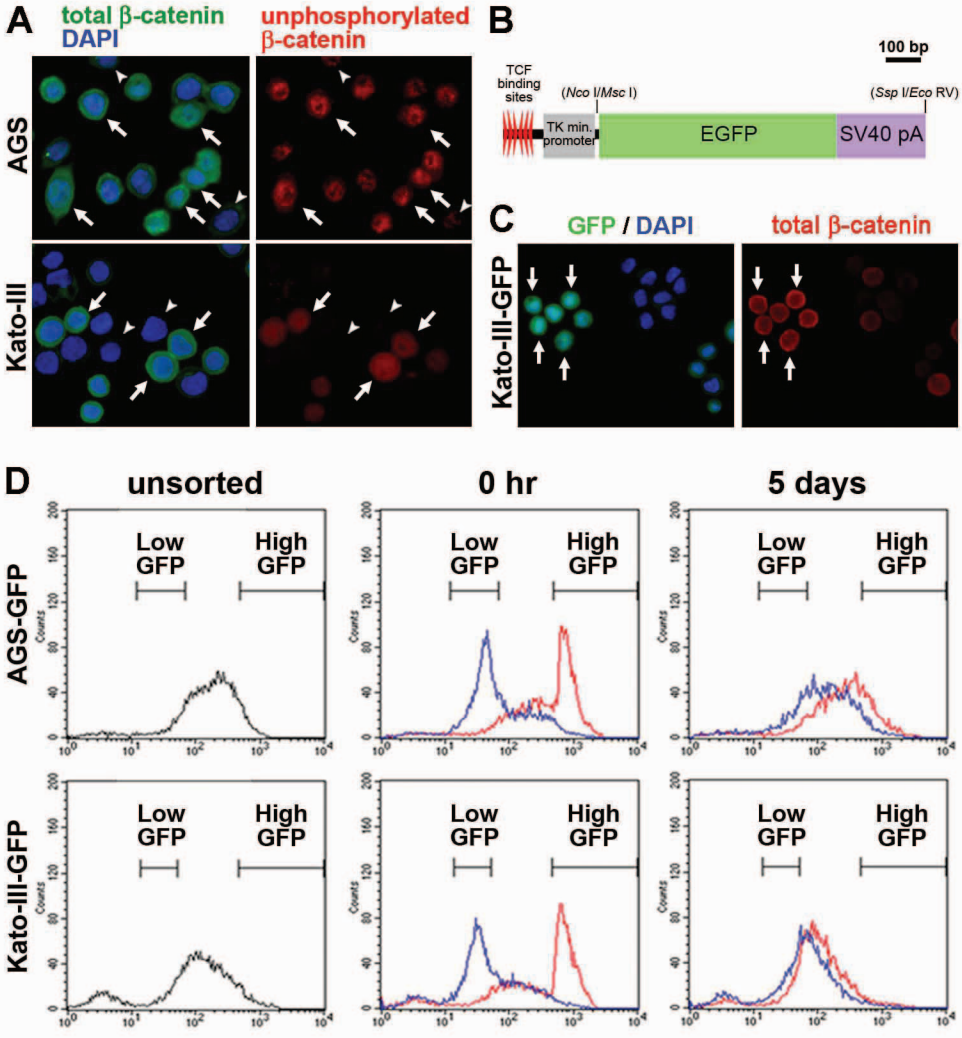
A
total β-catenin
DAPI
unphosphorylated
β-catenin
AGS
Kato-III
B
100 bp
TCF
binding
sites
(Nco I/Msc I)
(Ssp I/Eco RV)
TK min.
promoter
EGFP
SV40 pA
C
GFP / DAPI
total β-catenin
Kato-III-GFP
D
unsorted
0 hr
5 days
AGS-GFP
Kato-III-GFP
Low
GFP
High
GFP
Counts

Figure 4

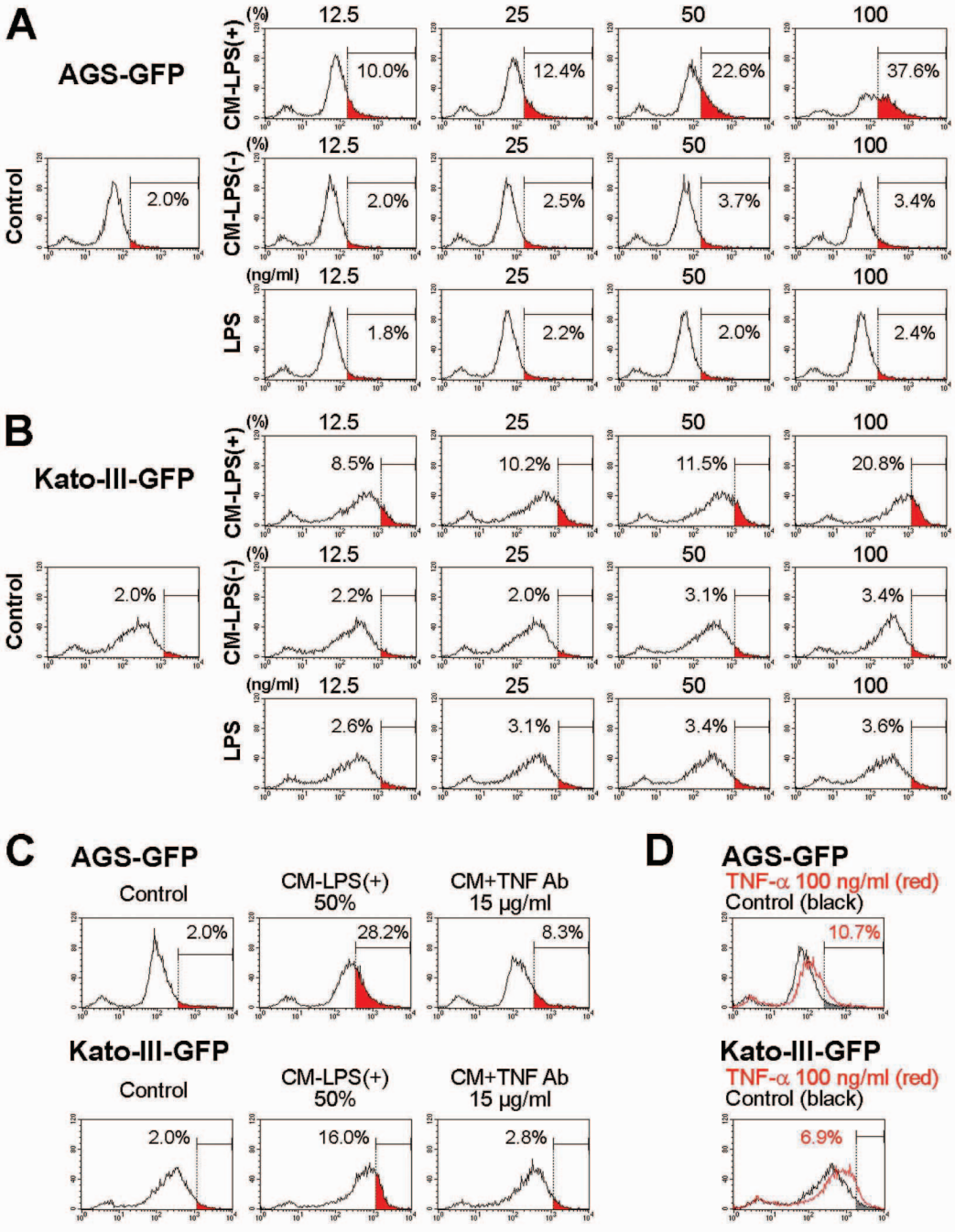
A
AGS-GFP
Control
2.0%
(%)
CM-LPS(+)
12.5
10.0%
25
12.4%
50
22.6%
100
37.6%
CM-LPS(-)
12.5
2.0%
25
2.5%
50
3.7%
100
3.4%
(ng/ml)
LPS
12.5
1.8%
25
2.2%
50
2.0%
100
2.4%
B
Kato-III-GFP
Control
2.0%
(%)
CM-LPS(+)
12.5
8.5%
25
10.2%
50
11.5%
100
20.8%
CM-LPS(-)
12.5
2.2%
25
2.0%
50
3.1%
100
3.4%
(ng/ml)
LPS
12.5
2.6%
25
3.1%
50
3.4%
100
3.6%
C
AGS-GFP
Control
2.0%
CM-LPS(+) 50%
28.2%
CM+TNF Ab 15 μg/ml
8.3%
Kato-III-GFP
Control
2.0%
CM-LPS(+) 50%
16.0%
CM+TNF Ab 15 μg/ml
2.8%
D
AGS-GFP
TNF-α 100 ng/ml (red)
Control (black)
10.7%
Kato-III-GFP
TNF-α 100 ng/ml (red)
Control (black)
6.9%

Figure 5

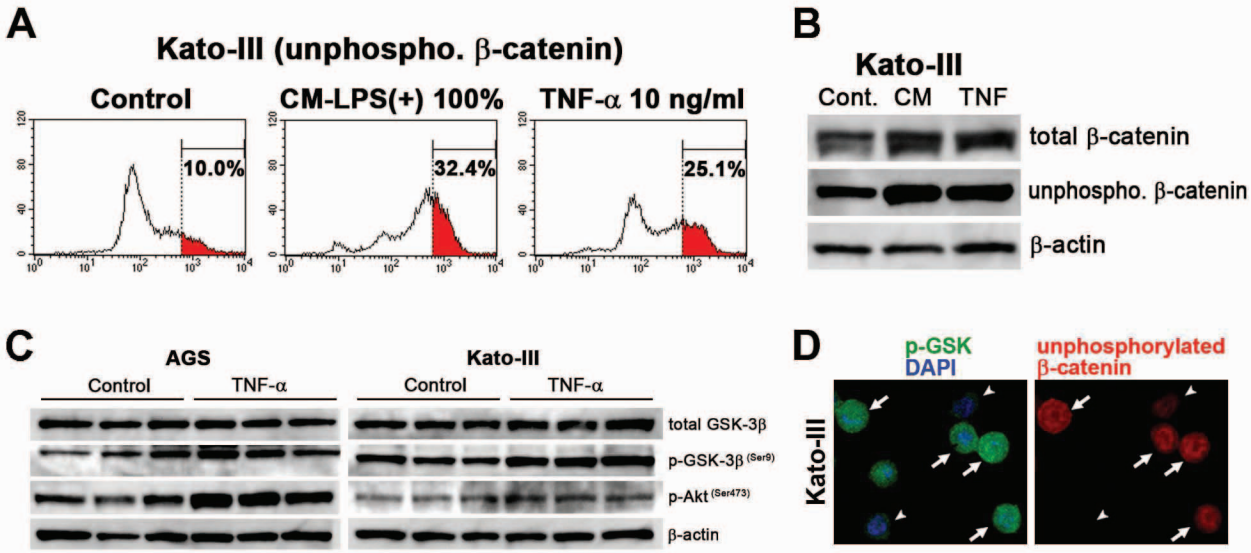
A
Kato-III (unphospho. β-catenin)
Control
CM-LPS(+) 100%
TNF-α 10 ng/ml
10.0%
32.4%
25.1%
B
Kato-III
Cont. CM TNF
total β-catenin
unphospho. β-catenin
β-actin
C
AGS
Kato-III
Control
TNF-α
Control
TNF-α
total GSK-3β
p-GSK-3β (Ser9)
p-Akt (Ser473)
β-actin
D
p-GSK
DAPI
unphosphorylated
β-catenin
Kato-III

Figure 6

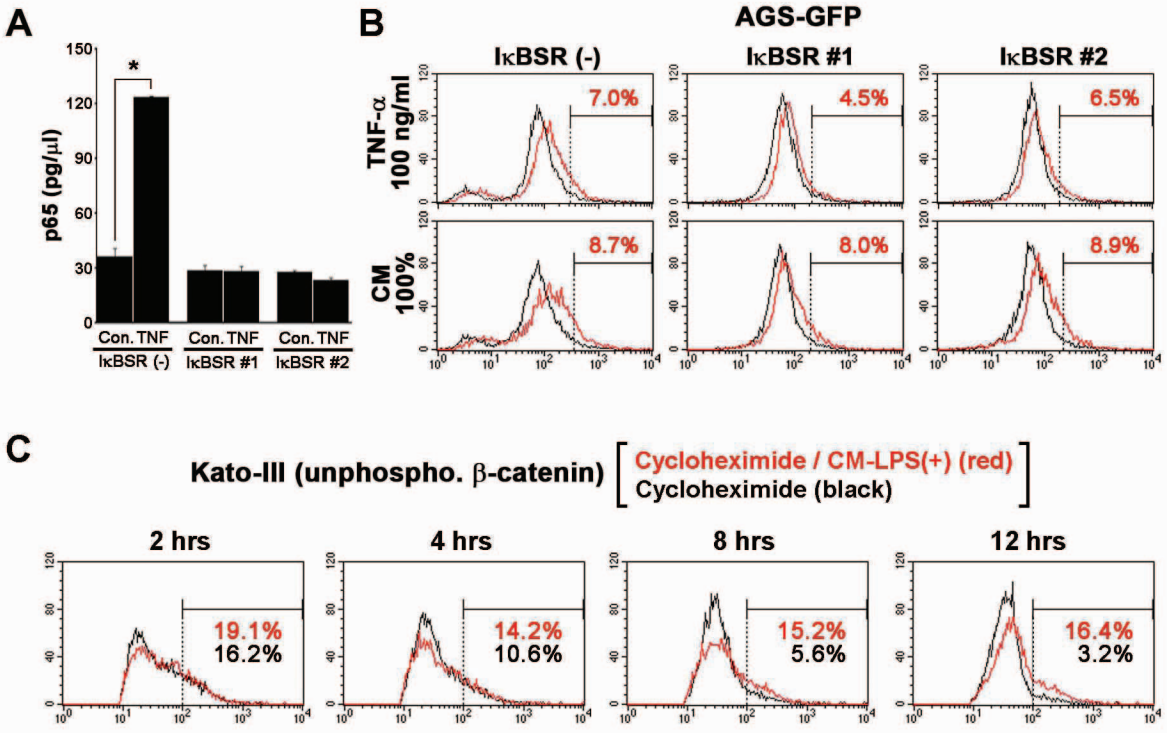
A
p65 (pg/μl)
150
120
90
60
30
0
*
Con. TNF
IκBSR (-)
Con. TNF
IκBSR #1
Con. TNF
IκBSR #2
B
AGS-GFP
IκBSR (-)
IκBSR #1
IκBSR #2
TNF-α 100 ng/ml
CM 100%
7.0%
4.5%
6.5%
8.7%
8.0%
8.9%
C
Kato-III (unphospho. β-catenin)
Cycloheximide / CM-LPS(+) (red)
Cycloheximide (black)
2 hrs
4 hrs
8 hrs
12 hrs
19.1%
16.2%
14.2%
10.6%
15.2%
5.6%
16.4%
3.2%

Figure 7

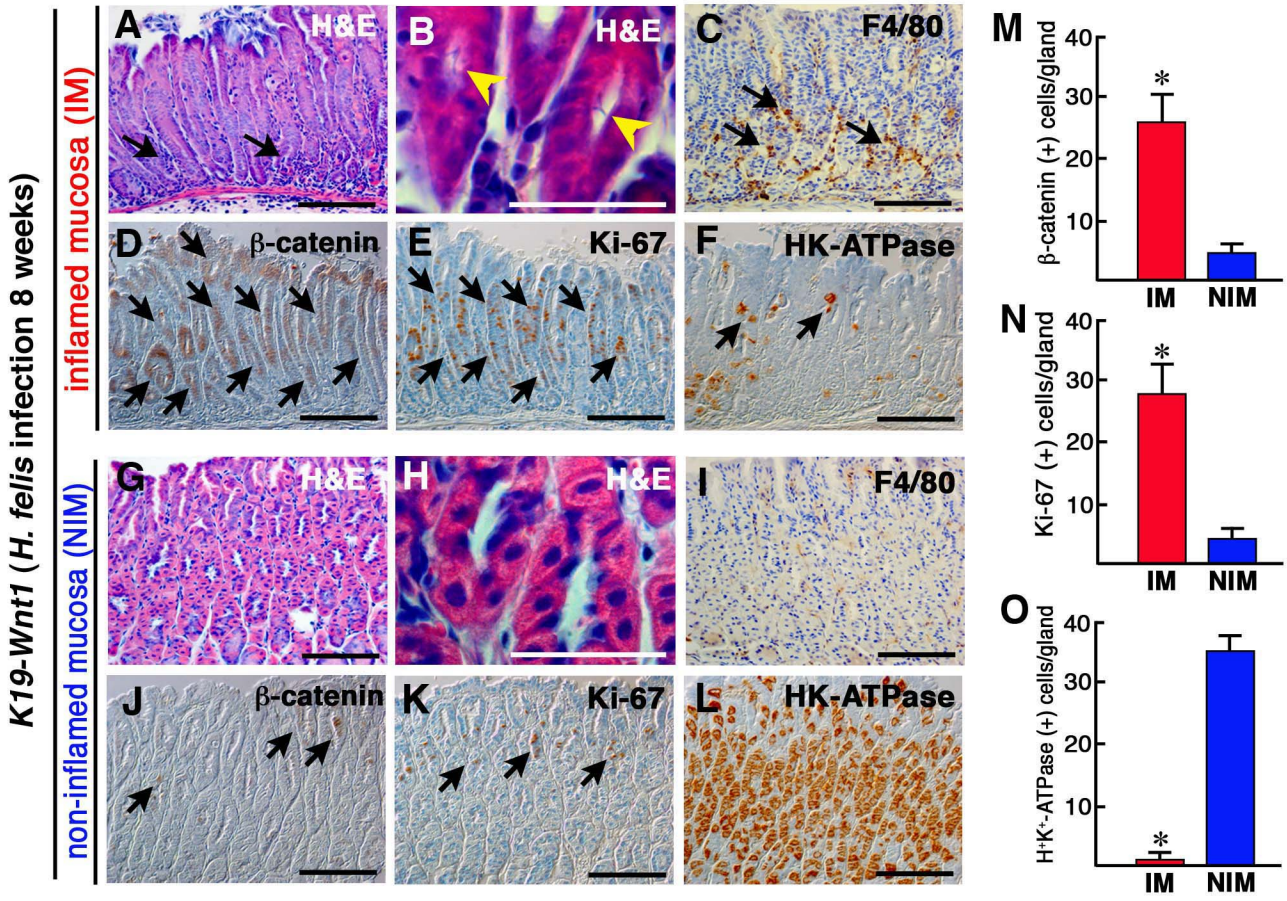
K19-Wnt1 (H. felis infection 8 weeks)
inflamed mucosa (IM)
non-inflamed mucosa (NIM)
A H&E
B H&E
C F4/80
D β-catenin
E Ki-67
F HK-ATPase
G H&E
H H&E
I F4/80
J β-catenin
K Ki-67
L HK-ATPase
M
β-catenin (+) cells/gland
40
30
20
10
*
IM
NIM
N
Ki-67 (+) cells/gland
40
30
20
10
*
IM
NIM
O
H+K+-ATPase (+) cells/gland
40
30
20
10
*
IM
NIM

Figure 8

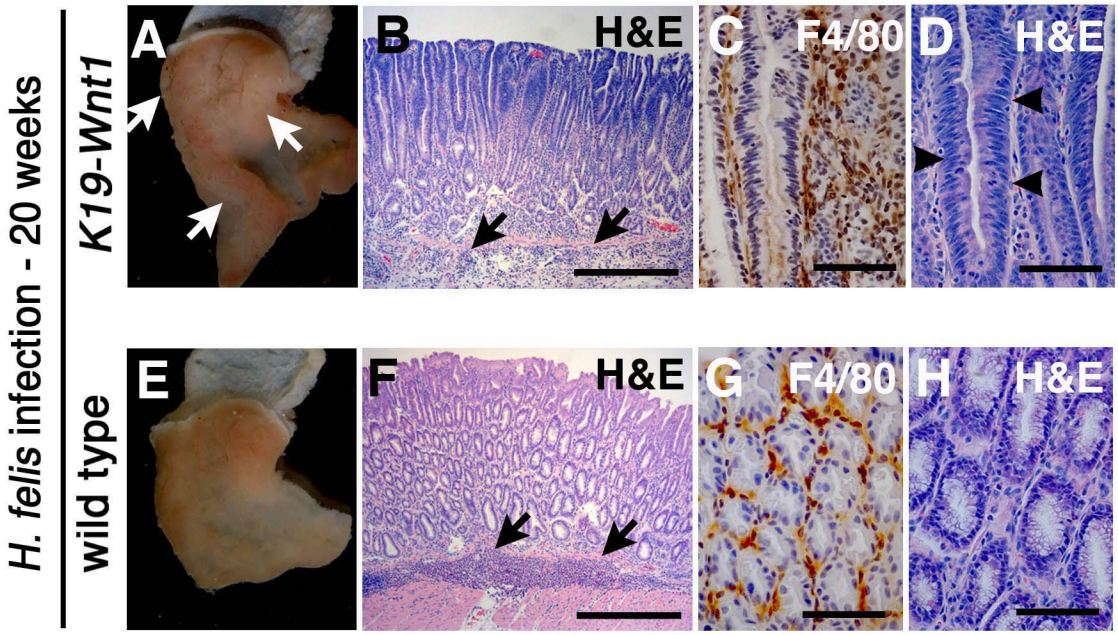
H. felis infection - 20 weeks
K19-Wnt1
wild type
A
B
H&E
C
F4/80
D
H&E
E
F
H&E
G
F4/80
H
H&E